# Coulomb oscillations in the electron thermal conductance of a dot in the linear regime

X. Zianni
*Department of Applied Sciences, Technological Educational Institution of Chalkida, 34400 Psachna, Greece*
(Received 28 March 2006; revised manuscript received 29 September 2006; published 30 January 2007)

The electron thermal conductance, $\kappa$, of a dot has been calculated in the regime of weak coupling with two electrode leads within a linear response theory. We discuss the effect of the interplay between the charging energy, the thermal energy, and the confinement in the Coulomb oscillations of $\kappa$. Hence, we consider three energy regions: the quantum limit, where quantum confinement dominates over the thermal energy; the classical regime, where the discreteness of the energy spectrum is screened by the thermal energy; and the intermediate energy region. In the quantum limit, the periodicity of the oscillations of the electron thermal conductance is the same as the Coulomb-blockade oscillations of the conductance, $G$. Analytical expressions have been obtained for $\kappa$ and $G$ in the cases of nondegenerate and for doubly degenerate energy spectrum. The obtained dependence of $\kappa$ on the energy level spacing and the thermal energy explicitly shows that quantum confinement is responsible for the fast decrease of the electron thermal conductance of a dot. It is found that degeneracies in the energy spectrum of a dot are opposed to the decrease of the electron thermal conduction due to quantum confinement. It is shown that an external field that raises the degeneracies causes a considerable enhancement in $\kappa$. In the classical and in the intermediate regimes, the electron thermal conductance shows distinct behavior at low and high temperatures. In the classical regime, Coulomb blockade oscillations are shown at low temperatures and simple formulas are obtained for $\kappa$ and $G$. The Wiedermann-Franz law holds at the peaks of $\kappa$ and $G$. The temperature dependence of $\kappa$ and $G$ has been calculated up to the limit where transport occurs through two isolated barriers. The relation between $\kappa$ and $G$ with increasing thermal energy is discussed.

DOI: 10.1103/PhysRevB.75.045344 PACS number(s): 73.63.Kv, 73.23.Hk, 73.50.Lw

## I. INTRODUCTION

For the past two decades structures based on semiconductor quantum dots have attracted a lot of research interest due to the opportunity to engineer their electronic properties. Until recently, most attention has been focused on possible electronics and optoelectronics applications. Recently, there is an increased interest in studying the thermal properties in quantum dot structures.[1–16] An intriguing ability of independent control of electronic and thermal properties in quantum dots stimulated a great deal of interest devoted mainly to possible thermoelectric applications. An increase in thermoelectric figure of merit in quantum dots is anticipated due to modification of its thermal properties in addition to the electronic ones. All of this motivates current interest in understanding and modeling quantum dot thermal properties. In recent years, there have been proposed thermoelectric applications of quantum dot superlattices made of different material systems as well as periodic arrays of dots.[4,8–15] In all theoretical and experimental studies the crucial role of the values of the electrical and the thermal conductivities in these nanostructures has been pointed out. Relative large values of the carrier mobility have been attributed either to hopping type or to band type conduction. Reduced thermal conductivity has been found and has been attributed to electron and phonon confinement. So, these structures seem promising for efficient thermoelectric devices and this explains the noticeable growing research interest in their properties. Other device applications are also expected. Nanocrystalline silicon has for instance recently proposed for designing efficient ultrasound emitter due to the measured low thermal conductivity relative to the bulk.[5] Moreover, heating effects in nanodevices are crucial in determining their operation characteristics so that this field is the subject of current technological research.

The thermoelectric phenomena have been adequately studied in the ballistic and in the diffusive transport regimes.[17–20] In the regime of single-electron tunneling, Coulomb blockade oscillations have been measured in the thermopower of a quantum dot.[16,21–24] The thermopower has been investigated theoretically in the sequential tunneling regime by Beenakker and Staring.[25] The cotunneling regime[26] and the crossover have been studied by Turek and Matveev.[27] In the case of a quantum dot strongly coupled to one lead, the thermopower has been investigated by Matveev and Andreev.[28] Recently, Koch *et al.* have extended these considerations to the thermopower of single molecules.[29] Heating effects also influence the properties of systems which exhibit Coulomb blockade effect which requires a study of heat transfer processes in these systems. Several experiments succeeded in measuring properties of heat transport in mesoscopic samples: Experimental tools based on the Coulomb blockade to measure accurately local temperatures in mesoscopic samples have been established.[30,31] It has been demonstrated that the heat conductance through one-dimensional phonon modes of a microbridge is quantized in low temperatures.[32] The universal heat conductance per mode is given by: $\pi^2 k_B^2 T/3h$. The same universal heat quantum is also found for carriers other than bosons.[33] The influence of the Coulomb blockade effect on the low-temperature thermal conductivity of a quantum dot with one-dimensional Luttinger liquid leads has been addressed in Ref. 34. The heat conduction through a Coulomb blockaded dot has been studied in Ref. 35 by analyzing the cooling mechanisms of the

 

electrons in the dot that are heated by an ac perturbation. Cooling is considered to be due to electron escape to the cold contacts and due to phonon emission. The cooling rate in the sequential tunneling regime is calculated for thermal energies greater than the energy levels spacing of the dot but low enough so that it can be assumed that the dot has either $N$ or $(N+1)$ electrons with finite probability.

In this work, the electron thermal conductance of a quantum dot weakly coupled to two electrode leads is calculated in the sequential tunneling regime within a linear response theory. It is presented a systematic study of the electron thermal conductance within this regime. Hence, the electron thermal conductance is studied for a wide range of values of the parameters that affect transport so that the effects of the charging energy, the thermal energy, the quantum confinement, and the energy spectrum degeneracy become evident. The Coulomb interaction is treated within the framework of the "orthodox model" of single-electron tunneling.[36] Two major simplifications of this model are that virtual tunneling processes are neglected and that the electrostatic energy is described by the classical charging energy: $(Ne)^2/2C$, where $N$ is the number of electrons in the dot and $C$ is the capacitance of the surroundings.

About the first simplification: In the sequential tunneling regime rate equations are used to describe the transport through the quantum dot.[37–39] This approach destroys the coherence phenomena associated with transport, since it neglects nonresonant quantum virtual processes, under the assumption that the resonant decay widths, $\Gamma$, are much smaller than both the thermal energy, $k_BT$, and the energy separation between the quantum dot resonances, a condition often met by experiments in nearly isolated dots.[23,40] Coherent versus sequential description of tunneling has been discussed for resonant tunneling diodes[41–43] and more recently for quantum dots.[27,44] It is shown that whether quantum coherence leads to important corrections to the sequential tunneling picture that explain the experimental evidence, depends on the conditions of the experiment. Quantum virtual tunneling processes are significant whenever $k_BT$ becomes comparable with $\Gamma$. Furthermore, both the single particle level spacing and the decay widths fluctuate. Even if in average $\Delta \equiv \langle \Delta E \rangle \gg \langle \Gamma \rangle$, situations where $\Delta E$ is comparable to $\Gamma$ are possible.[45,46] In these cases, quantum corrections are important. When the condition $\Gamma/\Delta E \ll 1$ is always satisfied and not only in average, corrections to the conductance become indeed negligible.[40,47] In experiments[40] where special care is taken to discard from the statistical sample conductance peak heights that do not fulfill $\Gamma \ll k_BT$, good agreement with the standard sequential theory is obtained.

About the second simplification: The assumption that the charging energy can be approximated by the classical charging energy requires that the screening length is much smaller than the size of the dot. This condition is fulfilled in typical metal structures, but not in all cases of semiconductors structures. In Ref. 48 self-consistent tight binding calculations have been compared with experimental results and it has been shown that for a nanocrystal of dielectric constant $\varepsilon_{in}$ that is embedded in a material of dielectric constant $\varepsilon_{out}$, when $\varepsilon_{in} >> \varepsilon_{out}$ the capacitive model can be applied with a good degree of accuracy. The effective capacitance can be adjusted in order to fulfill the relation $U \approx (Ne)^2/2C$ with $U$ defined as an average value.

Much theoretical work on the Coulomb blockade of the conductance in a double-junction geometry deals with modifications of the orthodox model which are required when either or both of the above conditions are not fulfilled. In the present study we stay within the orthodox model to see what effects this model predicts for the electron thermal conductance of a quantum dot. Coulomb effects are important and are expected to be visible in the transport coefficients when the charging energy dominates over the thermal energy and the electron confinement (measured by the energy level spacing $\Delta E$), i.e., $e^2/C > k_BT, \Delta E$. The charging energy of an isolated spherical dot of radius $R$ has been found[48] to be: $U(R) = \left(\frac{1}{\varepsilon_{out}} + \frac{0.79}{\varepsilon_{in}}\right)\frac{e^2}{R}$. This relation provides upper and lower bounds for the charging energy of a spherical dot that is surrounded by a complex dielectric medium. Because this medium cannot screen the electric fields more than a metal or less than vacuum, the bounds are given by the limits $\varepsilon_{out} \to 1$ (vacuum) and $\varepsilon_{out} \to \infty$ (metallic). The confinement energy of the dot is, within the quantum confinement model, determined by the dot radius $R$ and the electron mass $m$. Hence, the charging energy and the confinement energy are not independent variables because they both depend on the dot radius. However, their ratio may vary in a wide range of values depending of the values of the parameters $\varepsilon_{in}, \varepsilon_{out}$ and $m$. Hence, Coulomb effects can be important in quantum dots with discrete energy spectrum as well as in dots where the discreteness of the energy spectrum is negligible.

In the regime where Coulomb effects are important, the interplay between the thermal energy and the energy level spacing is reflected in the transport properties. Hence, we discuss the behavior of the electron thermal conductance in three regions: in the quantum limit ($\Delta E \gg k_BT$), where quantum confinement dominates over the thermal energy; in the classical regime ($\Delta E \ll k_BT$) where the discreteness of the energy spectrum is screened by the thermal energy; and in the intermediate energy region. It should be underlined that the names used for the above regimes, namely "quantum" and "classical," refer to the discrete or continuous character of the energy spectrum and the respective distribution functions in a quantum dot. Hence, quantum behavior due to charging effects is expected to be seen in all three energy regions. The theoretical model is described in Sec. II. The calculated electron thermal conductance is presented and discussed in Sec. III in the quantum limit, in the classical regime and in the intermediate region.

## II. THEORETICAL MODEL

We consider a double barrier tunnel junction. It consists of a quantum dot that is weakly coupled to two electron reservoirs via tunnel barriers. Each reservoir is assumed to be in thermal equilibrium and there are a voltage difference $V$ and a temperature difference $\Delta T$ between the two reservoirs. A continuum of electron states is assumed in the reservoirs that are occupied according to the Fermi-Dirac distribution:

$$f(E-E_F)=\left[1+\exp\left(\frac{E-E_F}{k_BT}\right)\right]^{-1}, \tag{2.1}$$

where the Fermi energy, $E_F$, in the reservoirs is measured relative to the local conduction band bottom.

The quantum dot is characterized by discrete energy levels $E_p$ $(p=1,2,\ldots)$ that are measured from the bottom of the potential well. Degeneracies can be included by multiple counting of the levels. Each level can be occupied by either one or zero electrons. It is assumed that the energy spectrum does not change by the number of electrons in the dot. The states in the dot are assumed to be weakly coupled to the states in the electrodes so that the charge of the quantum dot is well defined. We adopt the common assumption in the Coulomb blockade problems for the electrostatic energy $U(N)$ of the dot with charge $Q=-Ne$

$$U(N)=(Ne)^2/2C-N\phi_{ext}, \tag{2.2}$$

where $C$ is the effective capacitance between the dot and the reservoirs and $\phi_{ext}$ is the contribution of external charges.

The tunneling rates through the left and right barriers from level $p$ to the left and right reservoirs are denoted by $\Gamma_p^l$ and $\Gamma_p^r$, respectively. It is assumed that energy relaxation rates for the electrons are fast enough with respect to the tunneling rates so that we can characterize the state of the dot by a set of occupation numbers, one for each energy level. It is also assumed that inelastic scattering takes place exclusively in the reservoirs not in the dot. The transport through the dot can be described by rate equations.

The energy conservation condition for tunneling implies the following conditions:[37]

(1) for tunneling from an initial state $E^{i,l(r)}$ in the left (right) reservoir to a final state $p$ in the quantum dot

$$E^{i,l}(N)=E_p+U(N+1)-U(N)+\eta eV, \tag{2.3}$$

$$E^{i,r}(N)=E_p+U(N+1)-U(N)-(1-\eta)eV, \tag{2.4}$$

(2) for tunneling from an initial state $p$ in the quantum dot to a final state in the left (right) reservoir at energy $E^{f,l(r)}$

$$E^{f,l}(N)=E_p+U(N)-U(N-1)+\eta eV, \tag{2.5}$$

$$E^{f,r}(N)=E_p+U(N)-U(N-1)-(1-\eta)eV, \tag{2.6}$$

where $N$ is the number of electrons in the dot before the tunneling event, $\eta$ is the fraction of the voltage $V$ which drops over the left barrier. The energies in the reservoirs are measured from the local conduction-band bottom.

Due to the voltage difference $V$ and the temperature difference $\Delta T$ between the two reservoirs, electric, and thermal currents pass through the dot. The stationary current $I$ and the heat flux $Q$ through the left barrier are respectively given by the following equations:

$$I=-e\sum_{p=1}^{\infty}\sum_{\{n_i\}}\Gamma_p^l P(\{n_i\})\{\delta_{n_p,0}f(E^{i,l}(N)-E_F)-\delta_{n_p,1}[1-f(E^{f,l}(N)-E_F)]\}, \tag{2.7}$$

$$Q=\sum_{p=1}^{\infty}\sum_{\{n_i\}}\Gamma_p^l P(\{n_i\})\{\delta_{n_p,0}[E^{i,l}(N)-E_F]f(E^{i,l}(N)-E_F)-\delta_{n_p,1}[E^{f,l}(N)-E_F][1-f(E^{f,l}(N)-E_F)]\}, \tag{2.8}$$

where the second summation is over all possible combinations of occupation numbers $\{n_1,n_2,\ldots\}\equiv\{n_i\}$ of the energy levels in the quantum dot, each with stationary probability $P(\{n_i\})$. The numbers $n_i$ can take on only the values 0 and 1. The nonequilibrium probability distribution $P$ is a stationary solution of a kinetic equation. This has been solved in the linear regime by Beenakker[37] and his results are summarized in Appendix A. The solution is substituted in Eqs. (2.7) and (2.8) and the linearized expressions for the electric current $I$ and the heat flux $Q$ are obtained

$$I=\frac{e}{k_BT}\sum_{p=1}^{\infty}\sum_{N=1}^{\infty}\frac{\Gamma_p^l\Gamma_p^r}{\Gamma_p^l+\Gamma_p^r}P_{eq}(N)F_{eq}(E_p/N)\times[1-f(\varepsilon_p-E_F)]\left[eV-\frac{\Delta T}{T}(\varepsilon_p-E_F)\right], \tag{2.9}$$

$$Q=-\frac{1}{k_BT}\sum_{p=1}^{\infty}\sum_{N=1}^{\infty}\frac{\Gamma_p^l\Gamma_p^r}{\Gamma_p^l+\Gamma_p^r}P_{eq}(N)F_{eq}(E_p/N)[1-f(\varepsilon_p-E_F)]\times(\varepsilon_p-E_F)\left[eV+\frac{\Delta T}{T}(\varepsilon_p-E_F)\right]. \tag{2.10}$$

Where $\varepsilon_p\equiv E_p+U(N)-U(N-1)$. $P_{eq}(N)$ is the probability that the quantum dot contains $N$ electrons in equilibrium and $F_{eq}(E_p/N)$ is the conditional probability in equilibrium that level $p$ is occupied given that the quantum dot contains $N$ electrons. The above equilibrium probabilities are respectively defined[37] as

$$P_{eq}(N)=\sum_{\{n_i\}}P_{eq}(\{n_i\})\delta_{N,\Sigma_i n_i}, \tag{2.11}$$

$$F_{eq}(E_p/N)=\frac{1}{P_{eq}(N)}\sum_{\{n_i\}}P_{eq}(\{n_i\})\delta_{n_p,1}\delta_{N,\Sigma_i n_i}. \tag{2.12}$$

$P_{eq}(\{n_i\})$ is the Gibbs distribution in the grand canonical ensemble

$$P_{eq}(\{n_i\})=Z^{-1}\exp\left[-\frac{1}{k_BT}\left(\sum_{i=1}^{\infty}E_in_i+U(N)-NE_F\right)\right], \tag{2.13}$$

where $N\equiv\Sigma_i n_i$ and Z is the partition function

$$Z=\sum_{\{n_i\}}\exp\left[-\frac{1}{k_BT}\left(\sum_{i=1}^{\infty}E_in_i+U(N)-NE_F\right)\right]. \tag{2.14}$$

In the regime of linear response, the current $I$ and the heat flux $Q$ are related to the applied voltage difference $V$ and the temperature difference $\Delta T$ by the equations[17]

$$\begin{pmatrix} I \\ Q \end{pmatrix} = \begin{pmatrix} G & L \\ M & K \end{pmatrix} \begin{pmatrix} V \\ \Delta T \end{pmatrix}. \tag{2.15}$$

The thermoelectric coefficients are related by Onsager relation that in the absence of a magnetic field is

$$M = -LT. \tag{2.16}$$

Equation (2.15) can be reexpressed with the current $I$ rather than the voltage $V$ as an independent variable

$$\begin{pmatrix} V \\ Q \end{pmatrix} = \begin{pmatrix} R & S \\ \Pi & -\kappa \end{pmatrix} \begin{pmatrix} I \\ \Delta T \end{pmatrix}. \tag{2.17}$$

The resistance $R$ is the reciprocal of the isothermal conductance $G$. The thermopower $S$ is defined as

$$S \equiv -\left.\frac{V}{\Delta T}\right|_{I=0} = -L/G. \tag{2.18}$$

The Peltier coefficient is defined as

$$\Pi \equiv \left.\frac{Q}{I}\right|_{\Delta T=0} = M/G = ST, \tag{2.19}$$

where Eq. (2.16) has been used in the second equality.

Finally, the thermal conductance is defined as

$$\kappa \equiv -\left.\frac{Q}{\Delta T}\right|_{I=0} = -K\left(1 + \frac{S^2GT}{K}\right). \tag{2.20}$$

By comparison of the above definitions of the transport coefficients and the linearized expressions for $I$ and $Q$, the following expressions are extracted for the transport coefficients:

$$G = \frac{e^2}{k_BT}\sum_{p=1}^{\infty}\sum_{N=1}^{\infty} \gamma_p P_{eq}(N) F_{eq}(E_p/N)\{1 - f[E_p + U(N) - U(N-1) - E_F]\}, \tag{2.21}$$

$$S = -\frac{e}{k_BT^2G}\sum_{p=1}^{\infty}\sum_{N=1}^{\infty} \gamma_p [E_p + U(N) - U(N-1) - E_F] P_{eq}(N) F_{eq}(E_p/N)\{1 - f[E_p + U(N) - U(N-1) - E_F]\}, \tag{2.22}$$

$$K = -\frac{1}{k_BT^2}\sum_{p=1}^{\infty}\sum_{N=1}^{\infty} \gamma_p [E_p + U(N) - U(N-1) - E_F]^2 P_{eq}(N) F_{eq}(E_p/N)\{1 - f[E_p + U(N) - U(N-1) - E_F]\}, \tag{2.23}$$

where

$$\gamma_p \equiv \frac{\Gamma_p^l \Gamma_p^r}{\Gamma_p^l + \Gamma_p^r}. \tag{2.24}$$

The expressions (2.21) and (2.22) have been for the first time obtained in Refs. 25 and 37.

The above findings for the transport coefficients can be written in the following more general formalism for the transport coefficients:

$$G = L^{(0)}, \tag{2.25}$$

$$S = -\frac{1}{eT}(L^{(0)})^{-1}L^{(1)}, \tag{2.26}$$

$$K = \frac{1}{e^2T}L^{(2)}. \tag{2.27}$$

The electron thermal conductance, $\kappa$, is given by the expression

$$\kappa = \frac{1}{e^2T}[L^{(2)} - L^{(1)}(L^{(0)})^{-1}L^{(1)}], \tag{2.28}$$

where

$$L^{(\alpha)} = \frac{e^2}{k_BT}\sum_{p=1}^{\infty}\sum_{N=1}^{\infty} \frac{\Gamma_p^l \Gamma_p^r}{\Gamma_p^l + \Gamma_p^r}[E_p + U(N) - U(N-1) - E_F]^{(\alpha)} P_{eq}(N) F_{eq}(E_p/N)\{1 - f[E_p + U(N) - U(N-1) - E_F]\}. \tag{2.29}$$

## III. CALCULATED ELECTRON THERMAL CONDUCTANCE AND LIMITING EXPRESSIONS

Coulomb effects are important and are expected to be visible in the transport coefficients when the charging energy dominates over the thermal energy and the electron confinement (measured by the energy level spacing $\Delta E$), i.e., $e^2/C > k_BT, \Delta E$. In this regime, the interplay between the thermal energy and the energy level spacing is reflected in the transport properties. We discuss the behavior of the electron thermal conductance in three regions: in the quantum limit ($\Delta E \gg k_BT$), where quantum confinement dominates over the thermal energy; in the classical regime ($\Delta E \ll k_BT$) where the discreteness of the energy spectrum is screened by the thermal energy; and in the intermediate energy region. Moreover, it is always assumed that the thermal energy exceeds the width of the transmission resonance, i.e., $k_BT \gg h(\Gamma^r + \Gamma^l)$, so that the resonances are thermally broadened.

### A. Quantum limit

In the quantum limit, where $\Delta E \gg k_BT$, the discreteness of the energy spectrum of the quantum dot plays a predominant role. In this limit, the term with $N = N_{min}$ gives the dominant contribution to the sums over $N$ in Eq. (2.29), where $N_{min}$ is the integer that minimizes the absolute value of

$$\Delta(N) = E_N + U(N) - U(N-1) - E_F. \tag{3.1}$$

Then, it is defined: $\Delta \equiv \Delta(N_{\min})$ and $\Delta_p \equiv E_p - E_{N_{\min}}$.

In this limit, simplified formulas can be obtained for the transport coefficients. For this, special care must be taken for the degeneracy of the energy spectrum. Hence, we discuss the behavior of the thermal conductance in two cases of energy spectrum: (a) with nondegenerate energy levels ($g=1$), and (b) with doubly degenerate energy levels ($g=2$), as in the case of spin degeneracy.

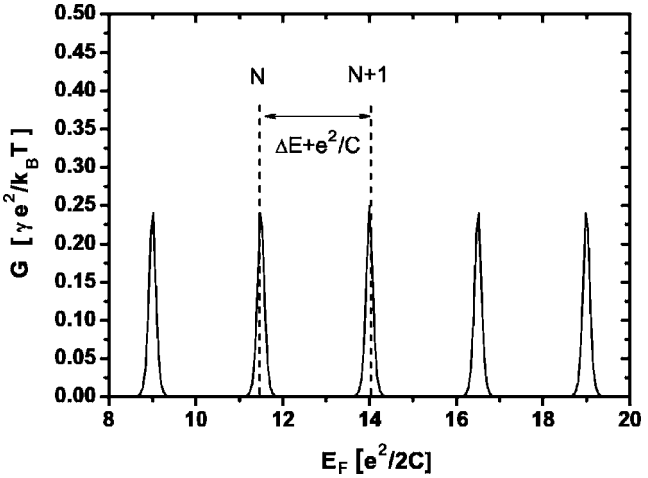


FIG. 1. Calculated conductance, $G$, for a series of equidistant, nondegenerate levels with separation $\Delta E=0.5\ e^2/2C$ and for $k_BT=0.05\ e^2/2C$. Level independent tunnel rates have been assumed.

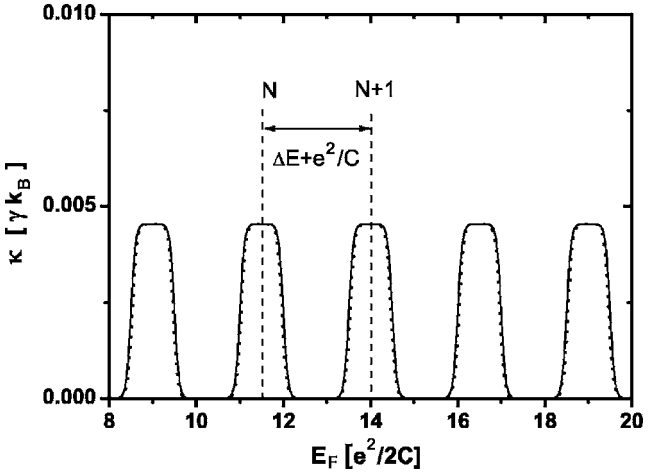


FIG. 2. Calculated electron thermal conductance, $\kappa$ (solid line), for a series of equidistant, nondegenerate levels with separation $\Delta E=0.5\ e^2/2C$ and for $k_BT=0.05\ e^2/2C$, i.e., ratio $\Delta E/k_BT=10$. Level independent tunnel rates have been assumed. For comparison, $\kappa^{QL}$ (dots) is also shown.

#### *1. Nondegenerate energy levels*

In the quantum limit, the distribution functions for nondegenerate energy levels can be approximated by the following expressions:

$$P_{eq}(N_{\min}) = \frac{1}{1+e^{\Delta/k_BT}}, \tag{3.2}$$

$$F_{eq}(E_p/N_{\min}) = \begin{cases} 1 & \text{for } p \leqslant N_{\min} \\ e^{-\Delta_p/k_BT} & \text{for } p > N_{\min}, \end{cases} \tag{3.3}$$

and

$$1-f(\Delta_p+\Delta) = \begin{cases} 1 & \text{for } p > N_{\min} \\ e^{(\Delta_p+\Delta)/k_BT} & \text{for } p < N_{\min} \\ \dfrac{e^{\Delta/k_BT}}{1+e^{\Delta/k_BT}} & \text{for } p = N_{\min}. \end{cases} \tag{3.4}$$

Using the above approximations in Eqs. (2.25)–(2.29), the following simplified formulas are obtained for $G$ and $\kappa$ for an equidistant energy levels spectrum ($E_p=p\Delta E$) and level-independent tunneling rates, i.e., $\Gamma_p^{l,r}=\Gamma^{l,r}$:

$$G^{QL} = \frac{e^2}{k_BT}\gamma\frac{1}{4\cosh^2(\Delta/2k_BT)}, \tag{3.5}$$

$$\kappa^{QL} = k_B\gamma\left(\frac{\Delta E}{k_BT}\right)^2\frac{e^{-\Delta E/k_BT}}{1+4\cosh^2(\Delta/2k_BT)e^{-\Delta E/k_BT}}, \tag{3.6}$$

where $\gamma \equiv \frac{\Gamma^l\Gamma^r}{\Gamma^l+\Gamma^r}$.

The calculated conductance is plotted in Fig. 1. For the values of the parameters used in Fig. 1, the curves computed from Eqs. (2.25) and (3.5) are indistinguishable and hence only one curve is shown. The calculated thermal conductance is plotted in Figs. 2 and 3, for two values of the ratio $\Delta E/k_BT$ in the quantum limit. The thermal conductance calculated from Eq. (3.6), $\kappa^{QL}$, is plotted together with the thermal conductance calculated from Eq. (2.28), $\kappa$, for comparison. In Fig. 2, where $\Delta E/k_BT=10$, $\kappa^{QL}$, and $\kappa$ are in perfect agreement. In Fig. 3, where $\Delta E/k_BT=5$, $\kappa^{QL}$ starts deviating from $\kappa$. This is because when the energy level spacing approaches the thermal energy, the quantum limit assumptions become less accurate. Hence, the quantum limit analytical formula holds satisfactorily when the energy level spacing is at least one order of magnitude higher than the thermal energy.

In Figs. 1–3, it is shown that in the quantum limit the conductance and the thermal conductance exhibit periodic Coulomb blockade oscillations. The peaks occur each time an extra electron enters in the dot and they are separated by intervals.

$$\Delta E_F = \Delta E + \frac{e^2}{C}. \tag{3.7}$$

The same periodicity has been found elsewhere[37] for the conductance, $G$, of quantum dots. This periodicity originates

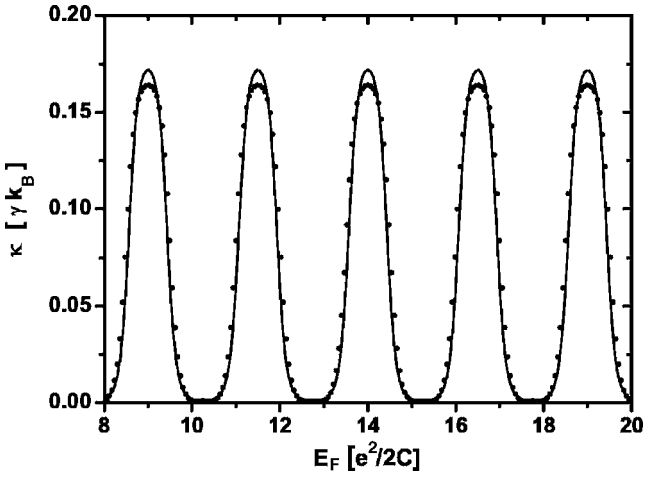


FIG. 3. As in Fig. 2 for $\Delta E/k_BT=5$, with: $\Delta E=0.5\ e^2/2C$ and $k_BT=0.1\ e^2/2C$.

from the fact that $|\Delta|$ is a periodic function of $E_F$ varying from zero to a maximum at intervals given by Eq. (3.7). $G$ and $\kappa$ depend on $\Delta$ through the same function of the hyperbolic cosine as it can be seen in Eqs. (3.5) and (3.6). The peaks in $\kappa$ and $G$ occur at the values of $E_F$ for which it holds: $\Delta=0$. The dependence of the maxima of $G$ and $\kappa$ on the characteristic parameters can be deduced from Eqs. (3.5) and (3.6), and it can be seen that the two transport properties exhibit different behavior: $G_{max}$ decreases linearly with increasing thermal energy and it is nearly independent of the energy level spacing; $\kappa_{max}$ depends on both the thermal energy and the energy level spacing through their ratio, $\Delta E/k_BT$, and it decreases rapidly with decreasing temperature and increasing energy level spacing.

In the thermal conductance behavior dominates the effect of quantum confinement due to the dependence on the ratio of the energy level spacing over the thermal energy, $\Delta E/k_BT$. This is analytically described by Eq. (3.6) and it is graphically shown by comparing the data plotted in Figs. 2 and 3. The electron thermal conductance of quantum dots decreases nearly exponentially with decreasing temperature. The dependence on the energy level separation, $\Delta E$, in Eq. (3.6) shows an equally fast decrease as the size of the dot decreases. Hence, it is explicitly shown that quantum confinement is responsible for the fast decrease of the electron thermal conductance. This behavior agrees with the observation that the thermal conductivity of a quantum dot is very small compared to that of bulk [e.g., Refs 1 and 4].

An equidistant energy level spectrum and energy independent tunneling rates have been assumed to deduce Eqs. (3.5) and (3.6). These assumptions are justified by the fact that in the quantum limit the main contribution to the conduction comes from a narrow energy region close to $E_p=E_{Nmin}$. $N_{min}$ increases by one each time a new conductance peak appears. Constant values for the energy level spacing and the tunneling rates can be used in the intervals of $E_F$ where $N_{min}$ is constant. The details of the energy spectrum and the energy dependence of the tunneling rates could be taken into account by assigning appropriate values for $N_{min}$ for each interval of $E_F$ in the quantum limit formulas. This would affect the position, the shape and the height of the peaks of the thermal conductance, as described by Eq. (3.6), resulting to a nonperiodic sequence of peaks.

### 2. Doubly degenerate energy levels

Let us now consider a twofold degeneracy of the energy levels (e.g., spin degeneracy). Coulomb interaction raises this degeneracy. The distribution functions depend on whether $N_{min}$ is odd or even and in the quantum limit they can be approximated by the following expressions:

**For odd** $N_{min}$

$$P_{eq}(N_{\min}) = \frac{1}{1+\frac{1}{2}e^{\Delta/k_BT}}, \tag{3.8}$$

$$F_{eq}(E_p/N_{\min}) = \begin{cases} 1 & \text{for } p < N_{\min} \\ \frac{1}{2} & \text{for } p = N_{\min}, N_{\min}+1 \\ \frac{1}{2}e^{-\Delta_p/k_BT} & \text{for } p > N_{\min}+1, \end{cases} \tag{3.9}$$

and

$$1-f(\Delta_p+\Delta) = \begin{cases} 1 & \text{for } p > N_{\min}+1 \\ e^{(\Delta_p+\Delta)/k_BT} & \text{for } p < N_{\min} \\ \frac{e^{\Delta/k_BT}}{1+e^{\Delta/k_BT}} & \text{for } p = N_{\min}, N_{\min}+1, \end{cases} \tag{3.10}$$

**for even** $N_{min}$

$$P_{eq}(N_{\min}) = \frac{1}{1+2e^{\Delta/k_BT}}, \tag{3.11}$$

$$F_{eq}(E_p/N_{\min}) = \begin{cases} 1 & \text{for } p < N_{\min}-1 \\ 1 & \text{for } p = N_{\min}-1, N_{\min} \\ 2e^{-\Delta_p/k_BT} & \text{for } p > N_{\min}, \end{cases} \tag{3.12}$$

and

$$1-f(\Delta_p+\Delta) = \begin{cases} 1 & \text{for } p > N_{\min} \\ e^{(\Delta_p+\Delta)/k_BT} & \text{for } p < N_{\min}-1 \\ \frac{e^{\Delta/k_BT}}{1+e^{\Delta/k_BT}} & \text{for } p = N_{\min}-1, N_{\min}. \end{cases} \tag{3.13}$$

Using the above approximations in Eqs. (2.25)–(2.29), the following simplified formulas are obtained for $G$ and $\kappa$, for an equidistant energy levels spectrum and level-independent tunneling rates.

**For odd** $N_{min}$**:**

$$G = \frac{e^2}{k_BT}\gamma\left[\frac{2(1+e^{\Delta/k_BT})}{2+e^{\Delta/k_BT}}\frac{1}{4\cosh^2(\Delta/2k_BT)} + \frac{2e^{\Delta/k_BT}}{2+e^{\Delta/k_BT}}e^{-\Delta E/k_BT}\right], \tag{3.14}$$

and

$$\kappa = k_B\gamma\frac{2(2e^{\Delta/k_BT}+1)}{2+e^{\Delta/k_BT}}\left(\frac{\Delta E}{k_BT}\right)^2 \times \frac{e^{-\Delta E/k_BT}}{1+4\cosh^2(\Delta/2k_BT)e^{-\Delta E/k_BT}+(1+e^{\Delta/k_BT})e^{-\Delta E/k_BT}}. \tag{3.15}$$

The second term in the parenthesis of (3.14) and the third term in the denominator of (3.15) can be neglected for energies below the edge of the quantum limit and it is obtained

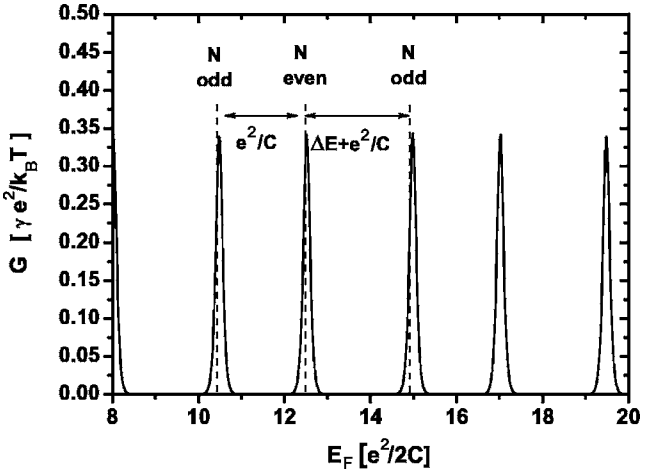


FIG. 4. Calculated conductance, $G$, for a series of equidistant, doubly degenerate levels with separation $\Delta E=0.5\ e^2/2C$ and for $k_BT=0.05\ e^2/2C$.

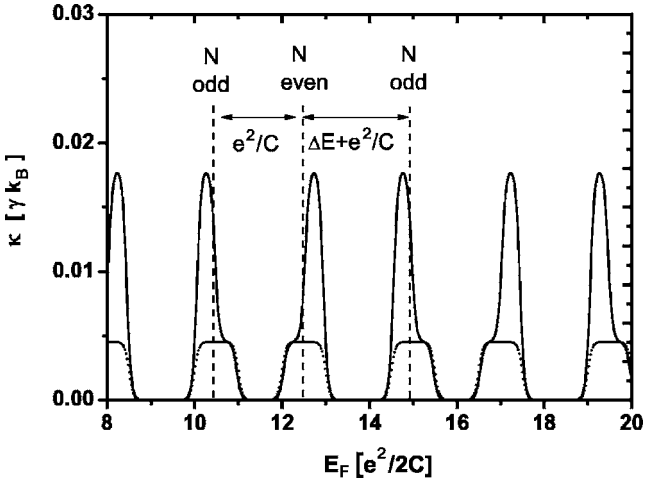


FIG. 5. Calculated electron thermal conductance, $\kappa$ (solid line), for a series of equidistant, doubly degenerate levels with separation $\Delta E=0.5\ e^2/2C$ and for $k_BT=0.05\ e^2/2C$. The dotted curve is for nondegenerate levels and is shown for comparison.

$$G^2 \approx \frac{2(1+e^{\Delta/k_BT})}{2+e^{\Delta/k_BT}}G^1, \tag{3.16}$$

and

$$\kappa^2 \approx \frac{2(2e^{\Delta/k_BT}+1)}{2+e^{\Delta/k_BT}}\kappa^1, \tag{3.17}$$

where the symbols $G^1$ and $\kappa^1$ denote the transport coefficients for $g=1$ and they are given by Eqs. (3.5) and (3.6). The symbols $G^2$ and $\kappa^2$ are for $g=2$.

**For even $N_{min}$:**

$$G=\frac{e^2}{k_BT}\gamma\left[\frac{2(1+e^{\Delta/k_BT})}{1+2e^{\Delta/k_BT}}\frac{1}{4\cosh^2(\Delta/2k_BT)}+\frac{2}{1+2e^{\Delta/k_BT}}e^{-\Delta E/k_BT}\right], \tag{3.18}$$

and

$$\kappa=k_B\gamma\frac{2(e^{\Delta/k_BT}+2)}{1+2e^{\Delta/k_BT}}\left(\frac{\Delta E}{k_BT}\right)^2 \times\frac{e^{-\Delta E/k_BT}}{1+4\cosh^2(\Delta/2k_BT)e^{-\Delta E/k_BT}+(1+e^{-\Delta/k_BT})e^{-\Delta E/k_BT}}. \tag{3.19}$$

Neglecting the third term in the denominators of the above two equations, it is obtained

$$G^2 \approx \frac{2(1+e^{\Delta/k_BT})}{1+2e^{\Delta/k_BT}}G^1, \tag{3.20}$$

and

$$\kappa^2 \approx \frac{2(e^{\Delta/k_BT}+2)}{1+2e^{\Delta/k_BT}}\kappa^1. \tag{3.21}$$

The calculated conductance and thermal conductance are shown in Figs. 4 and 5, respectively. In order to facilitate the comparison between the $g=1$ and the $g=2$ cases, the same parameters have been used in Figs. 1, 2, 4, and 5. The curves computed from the exact Eqs. (2.25) and (2.28) and the curves computed from the approximate equations are indistinguishable in Figs. 4 and 5. The Coulomb blockade peaks of the conductance and of the thermal conductance are non symmetric and they appear in doublets with mirror symmetry. The peaks of the conductance occur each time an extra electron enters the dot, when $\Delta=0$. The first peak of the doublet appears when an odd electron is added and the second peak appears when an even electron is added. The peaks are separated by $\Delta E_F=\Delta E+\frac{e^2}{C}$ when an odd electron enters the dot and by $\Delta E_F=\frac{e^2}{C}$ when an even electron enters the dot. In Fig. 5, $\kappa^1$ is plotted with a dotted line together with $\kappa^2$ so that the effect of spin degeneracy becomes more evident. (It should be noted that $\Delta E$ is the same for both $\kappa^1$ and $\kappa^2$, so that the amount of confinement is the same in the two cases.) It is due to the double degeneracy of the lower (upper) neighboring energy level, that offers an additional channel of conduction, that when an odd (even) electron is added, the left (right) half of the peak is enhanced. Due to spin degeneracy more channels of conduction contribute to the thermal conductance and give an enhancement of the thermal conductance. When temperature increases the asymmetry of the peaks is smoother, as it can be seen in Fig. 6 where the thermal conductance is plotted at a higher temperature.

The effect of raising the spin degeneracy (e.g., by applying a magnetic field) is shown in Fig. 7. The degenerate levels split to pairs of nondegenerate energy levels and their energy separation can be controlled by the external field. When the energy splitting is smaller than the energy separation due to confinement, the thermal conductance is considerably enhanced. This effect should be even more pronounced when $g>2$. Hence, degeneracies in the energy spectrum of a dot are opposed to the decrease of the electron thermal conduction due to quantum confinement.

### B. Classical regime

In the classical regime, $\Delta E \ll k_BT$, the discreteness of the energy spectrum of the quantum dot is screened by the ther-

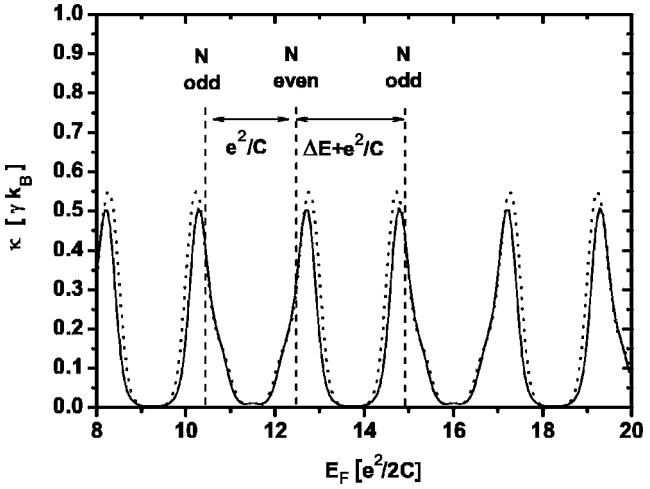


FIG. 6. Calculated electron thermal conductance, $\kappa$ (solid line), for a series of equidistant, doubly degenerate levels with separation $\Delta E=0.5\ e^2/2C$ and for $k_BT=0.1\ e^2/2C$. The dashed curve is calculated with the quantum limit expression.

mal energy and the energy spectrum can be treated as a continuum. In this limit, the electron distribution function $F_{eq}(E_p/N)$ can be approximated by the Fermi-Dirac distribution

$$F_{eq}(E_p/N) = f[E_p - \mu(N)], \tag{3.22}$$

where the chemical potential $\mu(N)$ is to be determined from the equation

$$\sum_{p=1}^{\infty} f[E_p - \mu(N)] = N. \tag{3.23}$$

The probability distribution $P$ takes the classical form

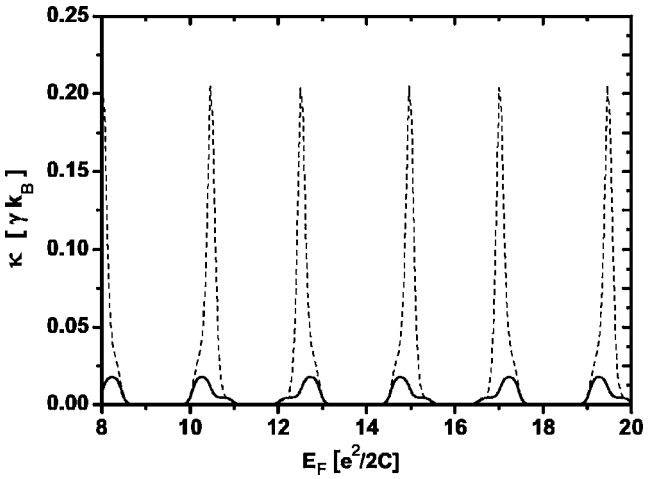


FIG. 7. The solid line is as in Fig. 5. The dashed line shows the effect of applying a field that raises the double degeneracy of the levels. Each level is split to a pair of levels with separation $\Delta E/5$.

$$P_{eq}^{cl}(N) = \frac{\exp\{-[U(N) + N(\bar{\mu} - E_F)]/k_BT\}}{\sum_N \exp\{-[U(N) + N(\bar{\mu} - E_F)]/k_BT\}}, \tag{3.24}$$

where $\bar{\mu}$ is the chemical potential of the dot in equilibrium. Then, the summation over $p$ in Eq. (2.29) may be replaced by integration over $E$. The algebra is given in Appendix B. The resulting expressions for the transport coefficients are

$$G = \frac{e^2\rho}{k_BT}\gamma\sum_{N=1}^{\infty} P_{eq}^{cl}(N)g[\Delta(N)], \tag{3.25}$$

$$S = -\frac{1}{2eT}\frac{\sum_{N=1}^{\infty} P_{eq}^{cl}(N)\Delta(N)g[\Delta(N)]}{\sum_{N=1}^{\infty} P_{eq}^{cl}(N)g[\Delta(N)]}, \tag{3.26}$$

$$K = -\frac{\rho\gamma}{k_BT^2}\sum_{N=1}^{\infty}\left[\frac{(\pi k_BT)^2 + \Delta^2(N)}{3}\right]P_{eq}^{cl}(N)g[\Delta(N)], \tag{3.27}$$

where $\rho$ is the density of states in the dot and $\Delta(N) \equiv U(N) - U(N-1) + \bar{\mu} - E_F$, where $\mu(N) \approx \text{const} = \bar{\mu}$ for all $N$ with significant probability. The above expressions are used in Eq. (2.20) to calculate $\kappa$.

For big charging energy, $\frac{e^2}{C} \gg k_BT$, the term with $N=N_{\min}$ gives the dominant contribution to the sums over $N$ in Eqs. (3.25)–(3.27), where $N_{\min}$ is the integer that minimizes the absolute value of $\Delta(N)$. Then, it is obtained

$$G = \frac{e^2\rho}{k_BT}\gamma P_{eq}^{cl}(N_{\min})g(\Delta_{\min}), \tag{3.28}$$

$$S = -\frac{1}{2eT}\Delta_{\min}, \tag{3.29}$$

$$K = -\frac{\rho\gamma}{k_BT^2}\left[\frac{(\pi k_BT)^2 + \Delta_{\min}^2}{3}\right]P_{eq}^{cl}(N_{\min})g(\Delta_{\min}). \tag{3.30}$$

The electron thermal conductance is given by the equation

$$\kappa = L_o\left[1 + \frac{1}{4\pi^2}\left(\frac{\Delta_{\min}}{k_BT}\right)^2\right]GT, \tag{3.31}$$

where $L_o = \frac{\pi^2}{3}\left(\frac{k_B}{e}\right)^2$ is the Lorentz number and $\Delta_{\min} \equiv \Delta(N_{\min})$.

When the thermal energy becomes big compared with the charging energy, $k_BT \gg \frac{e^2}{C}$, the amplitude of the Coulomb oscillations decreases and finally shrink. In this limit, it holds that: $g(\Delta) = k_BT$, and from Eqs. (3.25)–(3.27) and (2.20) it can be obtained

$$G_o = e^2\rho\gamma \tag{3.32}$$

and

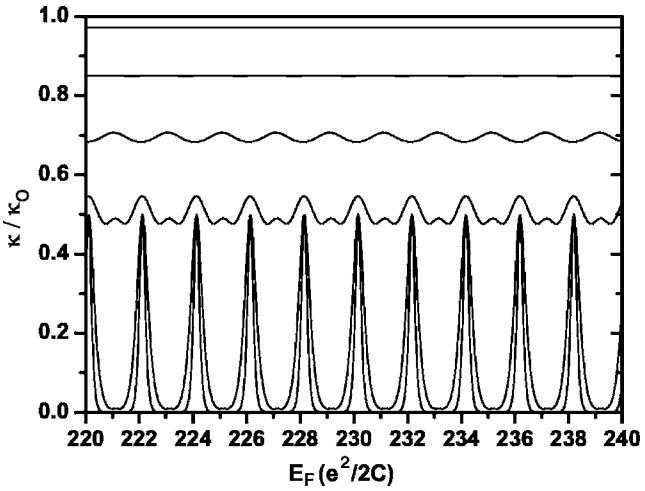


FIG. 8. Coulomb oscillations of the electron thermal conductance in the classical regime. The various curves are calculated for: $k_BT=0.05,0.1,0.3,0.5,1.0,5.0\ e^2/2C$. The lowest curve corresponds to the lowest thermal energy.

$$\kappa_o \approx \frac{\pi^2}{3} k_B \rho \gamma(k_B T). \tag{3.33}$$

Hence, in the limit of high temperatures, Eq. (3.32) implies that the resistance ($\equiv 1/G_o$) can be expressed as the sum of the tunnel resistances of the left ($1/e^2\rho\Gamma^l$) and right barriers ($1/e^2\rho\Gamma^r$).[37] Equation (3.33) can be written as: $\kappa_o = L_o G_o T$, i.e., the Wiedermann-Franz law holds in this limit.

The calculated thermal conductance in the classical regime is shown in Fig. 8 for varying thermal energy. The thermal conductance is normalized by $\kappa_o$. It can be seen that at low temperatures Coulomb blockade is exhibited. Then, the thermal conductance is given by Eq. (3.31). At the peaks, the periodicity of $\kappa$ is the same as that of the conductance, $G$. The periodicity of the Coulomb oscillations in the conductance in the classical limit is given by[37,51]

$$G = \frac{e^2\rho}{2} \gamma \frac{\Delta(N_{\min})/k_B T}{\sinh[\Delta(N_{\min})/k_B T]}. \tag{3.34}$$

According to Eq. (3.34), the peaks of $G$ occur when $\Delta(N_{\min})=0$. At low temperatures in the classical regime, the peaks of $G$ and $\kappa$ occur at the same Fermi energies as in the quantum limit (that is a low temperature regime). However, the shape of the peaks in the classical regime is different from that in the quantum limit, since the functional dependence $G$ and $\kappa$ on $\Delta(N_{\min})$ is different in the two regimes.

At the peaks of the thermal conductance, Eq. (3.31) becomes: $\kappa = L_o G T$, i.e., the Wiedermann-Franz law is valid. This is due to ballistic heat transfer at the peaks where the Coulomb barrier is suppressed. Away from the peaks it holds that $\Delta(N_{\min}) \neq 0$ and the relation between $\kappa$ and $G$ becomes

$$\kappa = L_{CB} G T, \tag{3.35}$$

with

$$L_{CB} = L_o \left[ 1 + \frac{1}{4\pi^2} \left( \frac{\Delta_{\min}}{k_B T} \right)^2 \right], \tag{3.36}$$

where $L_{CB}$ is a function of the Coulomb barrier and it has the periodicity of $\Delta^2_{\min}$, i.e., it becomes minimum (equal to zero) at the conductance peaks and maximum in between the peaks. Away from the peaks it holds: $L_{CB} > L_o$ and hence the heat transport is greater than the charge transport. The breakdown of the Wiedermann-Franz law at a conductivity threshold has been shown in other physics problems (see e.g., Refs 49 and 50). Here similar behavior is due to the Coulomb blockade effect. The maximum deviation from the Wiedermann-Franz law is at the threshold of conduction and the deviation decreases as the conduction peak is approached, where the Coulomb barrier is suppressed. In the presence of the Coulomb barrier 'hot' electrons contribute to the conduction.

Moreover, it is because $P^{cl}_{eq}(N)=0$ if $N \neq N_{\min}, N_{\min}-1$ that at the peaks of $\kappa$ and $G$, it holds that $P^{cl}_{eq}(N_{\min}) g(\Delta_{\min}) = k_B T/2$ and hence it is obtained

$$G_{\max} = e^2 \gamma \rho / 2 \tag{3.37}$$

and

$$\kappa_{\max} = \frac{\pi^2}{3} k_B \gamma(k_B T) \rho / 2. \tag{3.38}$$

Hence, at the peaks it holds that: $G_{\max}/G_o = 1/2$ and $\kappa_{\max}/\kappa_o = 1/2$. This relation between $\kappa_{\max}$ and $\kappa_o$ is also shown in the calculated thermal conductance data plotted in Fig. 8. This is due to destructive interference in the case of two coupled barriers that the conduction is limited by a factor of two relative to the case of two independent barriers in series.

When temperature increases, the thermal energy wins over the Coulomb barrier and conduction becomes possible at all values of $E_F$. Coulomb oscillations are observable until the charging energy becomes small compared with the thermal energy, $\frac{e^2}{C} \ll k_B T$. The effect of increasing thermal energy is shown in Fig. 8. The electron thermal conductance is non zero between the peaks, due to thermal broadening of the distribution functions that allows more channels to contribute to the conduction. As temperature increases, the contribution of the terms with $N=N_{\min}\pm 1$ to the sums over $N$ in Eqs. (3.25)–(3.27) becomes more and more important. At the peaks of $G$ it holds: $|\Delta(N)|_{\min}=0$, whereas at the peaks of $\kappa$ it holds: $|\Delta(N)|_{\max}=1$.

### C. Intermediate region

The intermediate region extends between the quantum limit and the classical regime. Here, the thermal energy and the levels spacing are comparable. The thermal energy is lower than the charging energy ($k_B T < e^2/C$) and Coulomb effects are non-negligible. Now, the summation over $p$ must be retained in Eqs. (2.25) and (2.29) and Eq. (2.28) has been used to calculate the electron thermal conductance. Even at high temperatures within this region, the discreteness of the energy spectrum is not being adequately screened by the

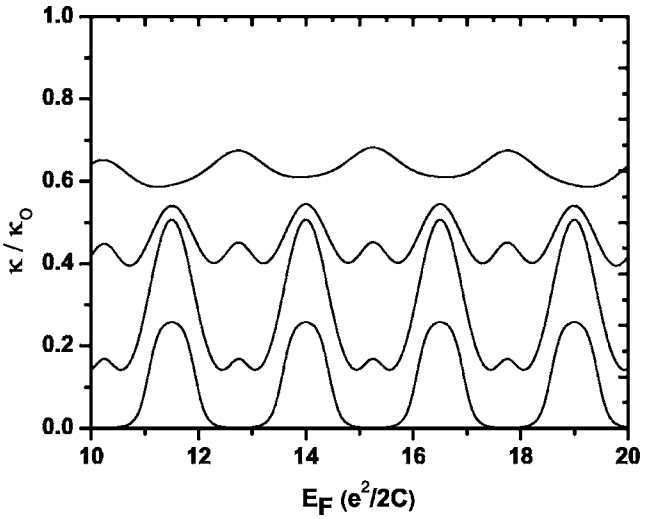


FIG. 9. Coulomb oscillations of the electron thermal conductance in the intermediate regime. The various curves are calculated for $\Delta E=0.5\ e^2/2C$ and for: $k_BT=0.1,0.3,0.4,0.5\ e^2/2C$. The lowest curve corresponds to the lowest thermal energy.

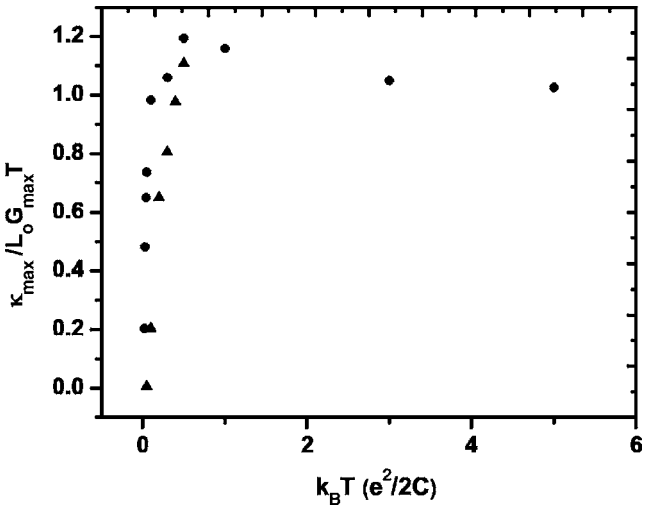


FIG. 10. The ratio $\kappa_{\max}/L_oG_{\max}T$ versus the thermal energy for two cases of confinement: for $\Delta E=0.1\ e^2/2C$ (dots) and for $\Delta E=0.5\ e^2/2C$ (triangles).

thermal energy and the summations cannot be changed to integrations.

The calculated electron thermal conductance is shown in Fig. 9 for $\Delta E=0.5\ e^2/2C$ for various temperatures. The lowest curve corresponds to the lowest temperature and it is at the edges of the quantum limit. At the highest temperature, the distribution functions can be satisfactorily approximated by their classical limits. In the intermediate region, the distribution functions deviate from the classical distributions and they are given by Eqs. (2.11) and (2.12). The behavior of the Coulomb oscillations with increasing temperature can be understood using similar arguments as in the classical regime. At the highest temperature, the distribution functions can be satisfactorily approximated by their classical limits. The onset of the classical region depends on the amount of confinement in the system. The intermediate region extends to higher temperatures for more amount of confinement, i.e., bigger $\Delta E$.

Finally, we comment on the relation between the thermal conductance and the conductance. For this, the ratio $\kappa_{\max}/L_oG_{\max}T$ is plotted versus the thermal energy in Fig. 10 for two cases of confinement: for $\Delta E=0.1\ e^2/2C$ (dots) and for $\Delta E=0.5\ e^2/2C$ (triangles). At low temperatures, quantum confinement that dominates over the thermal energy restricts the heat transport and the ratio is smaller than unity. Either in the quantum limit or in the intermediate region, quantum processes dominate in transport and cause deviations from the Wiedermann-Franz law that is restored at the onset of the classical regime, at the peaks of conduction. The Wiedermann-Franz law is expected to be restored faster with increasing temperature the weaker is the confinement. This is indeed found in the calculated data and it can be seen in Fig. 10 where the dots show a sharper increase than triangles with increasing thermal energy. In the classical regime, when only $N_{\min}$ contributes to transport the Wiedermann Franz law hold at the peaks. When temperature increases, the additional contributions of $N_{\min}+1$ and $N_{\min}-1$ favor at first the thermal conduction over the charge transport and the ratio becomes slightly bigger than unity. The Wiedermann-Franz law is again restored when due to thermal broadening all channels of conduction contribute equivalently to transport.

## ACKNOWLEDGMENTS

The present work has been cofunded by the European Community funds and by the National funds (E.P.E.A.E.K.), under the "Archimides" programme.

## APPENDIX A: ELECTRON PROBABILITY DISTRIBUTION

The nonequilibrium probability distribution $P$ is a stationary solution of the kinetic equation[25,37]

$$\frac{\partial}{\partial t}P(\{n_i\}) = 0 = -\sum_p P(\{n_i\})\delta_{n_p,0}\{\Gamma_p^l f_l[E^{i,l}(N)-E_F]+\Gamma_p^r f_r[E^{i,r}(N)-E_F]\} - \sum_p P(\{n_i\})\delta_{n_p,1}\{\Gamma_p^l[1-f_l(E^{i,l}(N)-E_F)]+\Gamma_p^r[1$$
$$-f_r(E^{i,r}(N)-E_F)]\} + \sum_p P(n_1,\ldots,n_{p-1},1,n_{p+1},\ldots)\delta_{n_p,0}\{\Gamma_p^l[1-f_l(E^{f,l}(N+1)-E_F) + \Gamma_p^r[1-f_r(E^{f,r}(N+1)-E_F)]\}$$
$$+\sum_p P(n_1,\ldots,n_{p-1},0,n_{p+1},\ldots)\delta_{n_p,1}\{\Gamma_p^l f_l[E^{i,l}(N-1)-E_F]+\Gamma_p^r f_r[E^{f,r}(N+1)-E_F]\}. \quad \text{(A1)}$$

The kinetic equation for the stationary distribution function is equivalent to the set of detailed balance equations (one for each $p=1,2,\ldots$)

$$\begin{aligned} &P(n_1,\ldots,n_{p-1},1,n_{p+1},\ldots)\{\Gamma_p^l[1-f_l(E^{f,l}(\tilde{N}+1)-E_F) \\ &\quad+\Gamma_p^r[1-f_r(E^{f,r}(\tilde{N}+1)-E_F)]\} \\ &\quad=P(n_1,\ldots,n_{p-1},0,n_{p+1},\ldots)\{\Gamma_p^l f_l(E^{i,l}(\tilde{N}-1)-E_F) \\ &\quad+\Gamma_p^r f_r(E^{f,r}(\tilde{N}+1)-E_F)\}, \end{aligned} \tag{A2}$$

with $\tilde{N}\equiv \sum_{i\neq p} n_i$.

In the linear response problem, it is substituted

$$P(\{n_i\}) \equiv P_{eq}(\{n_i\})[1+\Psi(\{n_i\})] \tag{A3}$$

into the detailed balance equation and it is expanded to first order in $\Delta T$ and $V$. It is defined

$$T_r \equiv T, T_l \equiv T+\Delta T$$

and

$$f(\varepsilon) \equiv [1+\exp(\varepsilon/k_BT)]^{-1},$$

where $\varepsilon \equiv E_p+U(\tilde{N}+1)-U(\tilde{N})-E_F$, so that it can be written

$$f_r(\varepsilon)=f(\varepsilon), \quad f_l(\varepsilon)=f(\varepsilon)-(\varepsilon\Delta T/T)f'(\varepsilon)+O(\Delta T)^2. \tag{A4}$$

Taking into account that:

$$1-f(\varepsilon) \equiv f(\varepsilon)e^{\varepsilon/k_BT}, \tag{A5}$$

$$\begin{aligned} &P_{eq}(n_1,\ldots,n_{p-1},1,n_{p+1},\ldots) \\ &\quad=P(n_1,\ldots,n_{p-1},0,n_{p+1},\ldots)e^{\varepsilon/k_BT}, \end{aligned} \tag{A6}$$

$$k_BTf'(\varepsilon)(1+e^{-\varepsilon/k_BT})=-f(\varepsilon), \tag{A7}$$

linearization of the detailed balance equation gives[25]

$$\begin{aligned} \Psi(n_1,\ldots,n_{p-1},1,n_{p+1},\ldots) &= \Psi(n_1,\ldots,n_{p-1},0,n_{p+1},\ldots) \\ &+\frac{eV}{k_BT}\left(\frac{\Gamma_p^r}{\Gamma_p^l+\Gamma_p^r}-\eta\right) \\ &+\frac{\varepsilon\Delta T}{k_BT^2}\frac{\Gamma_p^l}{\Gamma_p^l+\Gamma_p^r}. \end{aligned} \tag{A8}$$

Equations (A3) and (A8), are used in Eqs. (2.7) and (2.8), to give the linearized expressions for the electric current $I$ and the heat flux $Q$ [Eqs. (2.9) and (2.10), respectively of the main text].

## APPENDIX B: THE TRANSPORT COEFFICIENTS IN THE CLASSICAL REGIME

In the classical regime, the summation over $p$ in Eqs. (2.29) may be replaced by integration over $E$, multiplied by the density of states $\rho(E)$ in the dot. If $k_BT \ll \bar{\mu}, E_F$, one may in general disregard the energy dependence of the density of states and of the tunnel rates. By using Eqs. (3.22)–(3.24), Eq. (2.21) gives

$$G=\frac{e^2\gamma\rho}{k_BT}\sum_{N=1}^{\infty}P_{eq}(N)\int_{-\infty}^{+\infty}f[\varepsilon-\Delta(N)][1-f(\varepsilon)]d\varepsilon, \tag{B1}$$

$$S=-\frac{e\gamma}{k_BT^2G}\sum_{N=1}^{\infty}P_{eq}(N)\int_{-\infty}^{+\infty}d\varepsilon\varepsilon f[\varepsilon-\Delta(N)][1-f(\varepsilon)], \tag{B2}$$

$$K=-\frac{\rho\gamma}{k_BT^2}\sum_{N=1}^{\infty}P_{eq}(N)\int_{-\infty}^{+\infty}d\varepsilon\varepsilon^2 f[\varepsilon-\Delta(N)][1-f(\varepsilon)], \tag{B3}$$

where $\varepsilon \equiv Ep+U(N)-U(N-1)-E_F$. The integrations in Eqs. (B1)–(B3) can be worked out analytically

$$g[\Delta(N)] \equiv \int_{-\infty}^{+\infty}d\varepsilon f[\varepsilon-\Delta(N)][1-f(\varepsilon)]=\frac{\Delta(N)}{1-e^{-\Delta(N)/k_BT}}, \tag{B4}$$

$$\int_{-\infty}^{+\infty}d\varepsilon\varepsilon f[\varepsilon-\Delta(N)][1-f(\varepsilon)]=\frac{1}{2}\Delta(N)g[\Delta(N)], \tag{B5}$$

$$\begin{aligned} &\int_{-\infty}^{+\infty}d\varepsilon\varepsilon^2 f[\varepsilon-\Delta(N)][1-f(\varepsilon)] \\ &\quad=\frac{[(\pi k_BT)^2+\Delta^2(N)]}{3}g[\Delta(N)]. \end{aligned} \tag{B6}$$

By substituting Eqs. (B4)–(B6) into Eqs. (B1)–(B3) respectively, the expressions (3.25)–(3.27) of the main text are obtained.


[1] T. C. Harman, M. P. Walsh, B. E. Laforge, and G. W. Turner, J. Electron. Mater. **34**, L19 (2005).

[2] A. Baladin, J. Nanosci. Nanotechnol. **5**, 1015 (2005).

[3] V. Sajfert, J. P. Setrajcic, S. Jacimovski, and B. Tosic, Physica E (Amsterdam) **25**, 479 (2005).

[4] Y. Bao, W. L. Liu, M. Shamsa, K. Alim, A. A. Balandin, and J. L. Liu, J. Electrochem. Soc. **152**, G432 (2005).

[5] T. Kihara, T. Harada, and N. Koshida, Jpn. J. Appl. Phys., Part 1 **44**, 4084 (2005).

[6] M. Shamsa, W. Liu, A. A. Balandin, and J. Liu, Appl. Phys. Lett. **87**, 202105 (2005).

[7] M. C. Llaguno, J. E. Fischer, A. T. Johnson, and J. Hone, Nano

Lett. **4**, 45 (2004).
[8] D. Vashaee and A. Shakouri, Phys. Rev. Lett. **92**, 106103 (2004).
[9] R. Yang and G. Chen, Phys. Rev. B **69**, 195316 (2004).
[10] A. A. Balandin and O. Lazarenkova, Appl. Phys. Lett. **82**, 415 (2003).
[11] J. L. Liu, A. Khitun, K. L. Wang, W. L. Liu, G. Chen, Q. H. Xie, and S. G. Thomas, Phys. Rev. B **67**, 165333 (2003).
[12] J. L. Liu, A. Khitun, K. L. Wang, T. Borca-Tasciuc, W. L. Liu, G. Chen, and D. P. Yu, J. Cryst. Growth **227–228**, 1111 (2001).
[13] A. Khitun, K. L. Wang, and G. Chen, Nanotechnology **11**, 327 (2000).
[14] J. P. Small, K. M. Perez, and P. Kim, Phys. Rev. Lett. **91**, 256801 (2003).
[15] A. V. Andreev and K. A. Matveev, Phys. Rev. Lett. **86**, 280 (2001).
[16] A. S. Dzurak, C. G. Smith, C. H. W. Barnes, M. Pepper, L. Martin-Moreno, C. T. Liang, D. A. Ritchie, and G. A. C Jones, Physica B **249**, 281 (1998).
[17] P. N. Butcher, in *Crystalline Semiconducting Materials and Devices*, edited by P. N. Butcher, N. H. March, and M. P. Tosi (Plenum Press, New York, 1986).
[18] C. W. J. Beenakker and H. van Houten, Solid State Phys. **44**, 1 (1991).
[19] S. Datta, *Electronic Transport in Mesoscopic Systems* (Cambridge University Press, Cambridge, 1995).
[20] D. K. Ferry and S. M. Goodnick, *Transport in Nanostructures* (Cambridge University Press, Cambridge, 1997).
[21] A. S. Dzurak, C. G. Smith, C. H. W. Barnes, M. Pepper, D. A. Ritchie, J. E. F. Frost, G. A. Jones, and D. G. Hasko, Solid State Commun. **87**, 1145 (1993).
[22] A. S. Dzurak, C. G. Smith, C. H. W. Barnes, M. Pepper, L. Martin-Moreno, C. T. Liang, D. A. Ritchie, and G. A. C Jones, Phys. Rev. B **55**, R10197 (1997).
[23] A. A. M. Staring, L. W. Molenkamp, B. W. Alpenaar, H. van Houten, O. J. A. Buyk, M. A. A. Mabesoone, C. W. J. Beenakker, and C. T. Foxon, Europhys. Lett. **22**, 57 (1993).
[24] L. W. Molenkamp, A. A. M. Staring, B. W. Alphenaar, H van Houten, and C. W. J. Beenakker, Semicond. Sci. Technol. **9**, 903 (1994).
[25] C. W. J. Beenakker and A. A. M. Staring, Phys. Rev. B **46**, 9667 (1992).
[26] D. V. Averin and Y. V. Nazarov, Phys. Rev. Lett. **65**, 2446 (1990).
[27] M. Turek and K. A. Matveev, Phys. Rev. B **65**, 115332 (2002).
[28] K. A. Matveev and A. V. Andreev, Phys. Rev. B **66**, 045301 (2002).
[29] J. Koch, F. von Oppen, Y. Oreg, and E. Sela, Phys. Rev. B **70**, 195107 (2004).
[30] J. P. Pekola, K. P. Hirvi, J. P. Kauppinen, and M. A. Paalanen, Phys. Rev. Lett. **73**, 2903 (1994).
[31] J. P. Kauppinen, K. T. Loberg, A. J. Manninen, J. P. Pekola, and R. A. Voutilainen, Rev. Sci. Instrum. **69**, 4166 (1998).
[32] K. Schwab, E. A. Henriksen, J. M. Worlock, and M. L. Roukes, Nature (London) **404**, 974 (2000).
[33] L. G. C. Rego and G. Kirczenow, Phys. Rev. B **59**, 13080 (1999).
[34] M. V. Moskalets, J. Exp. Theor. Phys. **90**, 842 (2000).
[35] D. M. Basko and V. E. Kravtsov, Phys. Rev. B **71**, 085311 (2005).
[36] D. V. Averin and K. K. Likharev, in *Mesoscopic Phenomena in Solids*, edited by B. L. Al'tshuler, P. A. Lee, and R. A. Webb (North-Holland, Amsterdam, 1991).
[37] C. W. J. Beenakker, Phys. Rev. B **44**, 1646 (1991).
[38] Y. Alhassid, Rev. Mod. Phys. **72**, 895 (2000).
[39] I. L. Aleiner, P. W. Brouwer, and L. I. Glazman, Phys. Rep. **358**, 309 (2002).
[40] A. G. Huibers, S. R. Patel, C. M. Marcus, P. W. Brouwer, C. I. Duruoz, and J. S. Harris, Phys. Rev. Lett. **81**, 1917 (1998).
[41] T. Weil and B. Vinter, Appl. Phys. Lett. **50**, 1281 (1987).
[42] M. Jonson and A. Grincwajg, Appl. Phys. Lett. **51**, 1729 (1987).
[43] S. Luryi, Superlattices Microstruct. **5**, 375 (1989).
[44] L. E. F. Foa Torres, C. H. Lewnkopf, and H. M. Pastawski, Phys. Rev. Lett. **91**, 116801 (2003).
[45] S. R. Patel, D. R. Stewart, C. M. Marcus, M. Gokcedag, Y. Alhassid, A. D. Stone, C. I. Duruoez, and J. S. Harris, Jr., Phys. Rev. Lett. **81**, 5900 (1998).
[46] J. A. Folk, C. M. Marcus, and J. S. Harris, Jr., Phys. Rev. Lett. **87**, 206802 (2001).
[47] R. Baltin, Y. Gefen, G. Hackenbroich, and H. A. Weidenmuller, Eur. Phys. J. B **10**, 119 (1999).
[48] Y. N. Niquet, C. Delerue, G. Allan, and M. Lannoo, Phys. Rev. B **65**, 165334 (2002).
[49] G. D. Guttman, E. Ben-Jacob, and D. J. Bergman, Phys. Rev. B **51**, 17758 (1995).
[50] H. Van Houten, L. W. Molenkamp, C. W. J. Beenakker, and C. T. Foxon, Semicond. Sci. Technol. **7**, B215 (1992).
[51] I. O. Kulik and R. I. Shekhter, Zh. Eksp. Teor. Fiz. **68**, 623 (1975); [Sov. Phys. JETP **41**, 308 (1975)].